Available online at www.CivileJournal.org

Civil Engineering Journal

Vol. 4, No. 7, July, 2018

# Performance of Post-Fire Composite Prestressed Concrete Beam Topped with Reinforced Concrete Flange

Nibras A. Harbi [a], Amer F. Izzet [a*]

[a] *Civil Engineering Department, College of Engineering, University of Baghdad, Iraq.*

Received 09 May 2018; Accepted 13 July 2018

**Abstract**

The performance of composite prestressed concrete beam topped with reinforced concrete flange structures in fire depends upon several factors, including the change in properties of the two different materials due to fire exposure and temperature distribution within the composition of the composite members of the structure. The present experimental work included casting of 12 identical simply supported prestressed concrete beams grouped into 3 categories, depending on the strength of the top reinforced concrete deck slab (20, 30, and 40 MPa). They were connected together by using shear connector reinforcements. To simulate the real practical fire disasters, 3 composite prestressed concrete beams from each group were exposed to high temperature flame of 300, 500, and 700°C, and the remaining beams were left without burning as reference specimens. Then, the burned beams were cooled gradually by leaving them at an ambient lab condition, after which the specimens were loaded until failure to study the effect of temperature on the residual beams serviceability, to determine the ultimate load-carrying capacity of each specimen in comparison with unburned reference beam, and to find the limit of the temperature for a full composite section to remain composite. It was found that the exposure to fire temperature increased the camber of composite beam at all periods of the burning and cooling cycle as well as the residual camber, along with reduction in beam stiffness and the modulus of elasticity of concrete in addition to decrease in the load-carrying capacity.

*Keywords:* Burning; Camber; Composite Section; Cooling.

## 1. Introduction

Several fire disasters have caused enormous damages to both life and property, and a number of studies have been performed on the structure following fire damage. However, these researches are either limited to the exterior of a structure or to testing components of it in the lab. Internal observations and flexural strength testing cannot be performed on the existing structure.

Concrete has often been taken for granted considering its non-combustible nature and the ability to function as a thermal barrier that prevents heat and fire spread [1]. The coefficient of thermal conductivity of concrete depends on the conductivity of its constituents, namely the cement paste and the aggregate [2]. After the exposure to fire, changes in the properties of concrete structure does not reverse, in contrast to that in case of steel structure, where cooling often restores most of its original state. Concrete deteriorations caused by changes in physical and chemical properties of the cement itself which have been irreversible transformations. These changes may use as an indicator to reflect the maximum exposure temperatures, depending on the post-fire examination of the state of concrete surface [3]. It should be noted that, although if there is no visible deterioration in some situations, a concrete structure may be considerably weakened after a fire. Up to 100°C further hydration of the cement concrete can be produce, resulting in an initial

* Corresponding author: amerfarouk@yahoo.com

http://dx.doi.org/10.28991/cej-0309198

increase in strength [4]. However, there is a loosening of inter-particle bond as a result of different coefficients of expansion [1]. Rapid temperature rise can result in vaporization of the entrapped water and loosening of the inter-particle bond, which occurs as a result of different coefficients of expansion, causing spalling. High rise rate of temperatures can result in the destruction of a concrete structure from severe spalling due to concrete expansion with rising temperatures, but higher temperatures also cause further shrinkage of the hardened concrete paste [5, 6]. These two opposite movements, forming micro cracks on cooling, as a result, complete recovery of deformation cannot be achieved. This process is complicated further when longitudinal expansion is restrained, as is often the case in prestressed concrete (PC) [7]. In general, high strength materials (concrete and steel reinforcements) prefer to be used in prestressed concrete members. It can be noted that, high strength concrete (HSC) which has considerably higher compressive strength than normal-strength concrete, but it is markedly less porous and moisture absorbent. This fact generally reduces the water content of cement, it also makes it harder for water vapor to escape during heating. It can however be argued that HSC is more prone to spalling due to its lower porosity, thereby contributing to the increased likelihood of high pressure developing within the concrete structure [8]. On another hand, the effect of high temperature on the reinforcing steel was by others [9, 10]. Youssef and Moftah [2] reported reinforcing steel is much more sensitive to high temperatures than concrete. It is generally believed that steel reinforcement bars need to be protected from exposure to temperatures in the excess of 250-300°C. This is due to the fact that steel with low carbon contents are known to exhibit "blue brittleness" between the temperatures of 200 and 300°C.

Fletcher et al. [12] concluded, concrete and steel exhibit similar thermal expansion at temperatures up to 400°C; however, higher temperatures result in significant expansion of steel as compared to that of concrete and, if temperatures of 700°C is attained, the load-bearing capacity of the steel reinforcement will reduce to about 20% of its design.

This research was conducted to study the behaviour of composite PC beams with reinforced concrete (RC) deck slab under and after the exposure to fire flame, find the limit of the temperature for the full composite section to remain composite (PC beam and the reinforced deck slab work as a composite beam), and study the residual ultimate capacity of the composite damaged PC beams with deck slab by fire flame.

## 2. Preparation of Experimental Beams

A composite PC beam composed of prestressed post-tensioned concrete beam (3300, 300, and 170 mm in length, depth, and width, respectively), topped with RC deck slab (400 mm width and 50 mm depth) with simply supported boundary condition at each end was selected and designed. Each PC beam passed through three stages of manufacturing: i) the lower part of each beam was cast and cured after reaching the specified concrete strength of 40 MPa at the age of 28 day. ii) The prestressing strand is inserted into the plastic tube fixed before casting the first stage of concrete of the lower part, a prestressing force of 120 kN is applied from one end by using a hydraulic jack, this value was selected to satisfy the limits of the ACI 318M-14 Code. The vertical deflection (camber) was 1.1 mm at the prestressing stage. iii) The final stage includes tying up of the prefabricated deck slab reinforcements with the headings of the shear connectors' reinforcements and pouring of concrete deck of 400 and 50 mm width and thickness, respectively.

## 3. Composite PC Beams Set Up

Each composite PC beam passed through three stages of manufacturing. First, the lower part of each beam had been cast and cured, after reaching the specified concrete strength (40MPa at 28 dayes), second stage began by applying prestressing force, then the final stage comprised casting the concrete deck slab (Figure 1).

In the second stage, prestressing force was applied by using single seven-wire low-relaxation strand, with 12.7 mm diameter and Grade 270. All beams were prestressed by applying same prestressing force of 120 kN. The prestressing process began by insertion the prestressing strand into the plastic tube which had been fixed before casting the first stage of concrete of the lower part, then the end bearing steel plate of 20 mm thick (170 and 100 mm, its length and width, respectively) with adequate grip was fixed at each end. After that, the prestressing force was applied from one end by using a hydraulic jack. The vertical upward deflection (camber), the strains at the top and bottom of the concrete surface and the strand strain were measured at the mid span of the beam at the prestressing stage to inspect the applied prestressing force.

Final stage included, tying up the prefabricated deck slab reinforcements with the headings of the shear connectors reinforcements. Finally, concrete deck of 400 and 50 mm its width and thickness, respectively, were poured.

## 4. Tested Composite PC Beams

The experimental program of this study included testing of 12 simply supported composite PC beams-RC deck slab (Table 1). Two categories of experimental tests were conducted on the PC beams as follows:

**Exposing To Fire Flam Test:** Three PC beams of each group were exposed to burning temperatures of 300, 500, or 700˚C for similar exposure period of 1 h after reaching the target temperature. After this period, the fire flame was turned

off, the manufactured furnace case was removed, and the PC beam was cooled gradually by the ambient air. The temperature was monitored using a digital thermometer reader equipped with thermocouple sensor wire type K fixed at mid-depth of the beam flange of the PC beam. In addition, a dial gauge of 0.01 mm/div. sensitivity was used to monitor the change in the camber at the top of the mid span of the PC beam (Figure 2).

**Load Application Test:** To find the behaviour and the residual ultimate strength, all PC beams including the unburned ones (reference PC beams), were loaded until failure after finishing the burning test category by applying static load downward through the mid-point of the stiffened I-section steel beam spreader (Figure 3). The results of these burned beams were compared with those of the unburned ones. Two types of measurements were adopted; mid-span deflection was measured by using a dial gauge of 0.01 mm/div. sensitivity, and another type of dial gauge of 0.001 mm/div. sensitivity was fixed laterally at the end of the beam to detect the end slip between the PC beam and the RC deck slab.

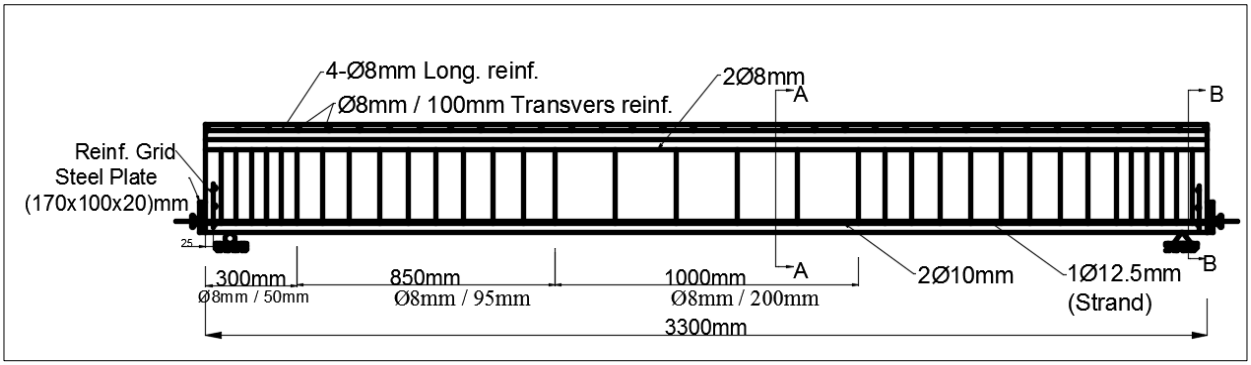


**PC beam side view**

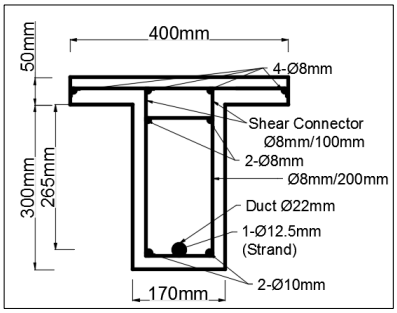


**Section A-A**

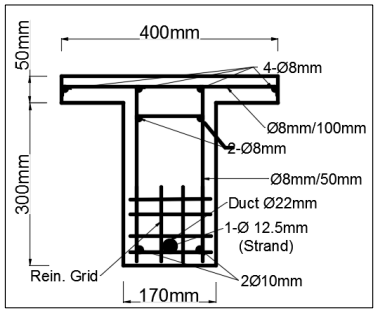


**Section B-B**

**Figure 1. Beam layout, dimensions and reinforcement details**

**Table 1. Composite PC beams with RC deck slab**

| Groups | Specimen | $f'_c$ for beam | $f'_c$ for deck slab | Burning temp ˚C |
|---|---|---|---|---|
| Group I | B1-F20-R | 40 | 20 | unburned |
| | B1-F20-300 | 40 | 20 | 300 |
| | B1-F20-500 | 40 | 20 | 500 |
| | B1-F20-700 | 40 | 20 | 700 |
| Group II | B2-F30-R | 40 | 30 | unburned |
| | B2-F30-300 | 40 | 30 | 300 |
| | B2-F30-500 | 40 | 30 | 500 |
| | B2-F30-700 | 40 | 30 | 700 |
| Group III | B3-F40-R | 40 | 40 | unburned |
| | B3-F40-300 | 40 | 40 | 300 |
| | B3-F40-500 | 40 | 40 | 500 |
| | B3-F40-700 | 40 | 40 | 700 |

Note: Cooling of the burned composite PC beams was performed gradually by leaving them at lab condition.

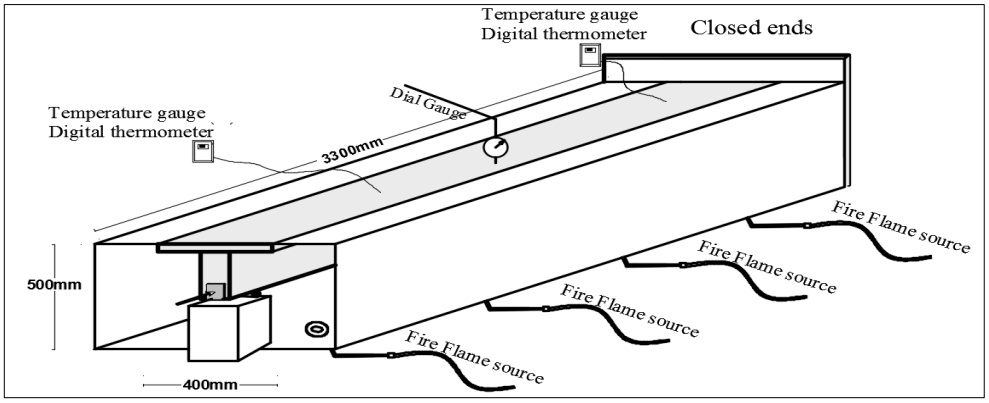


**Figure 2. Furnace schematic shape and burning process**

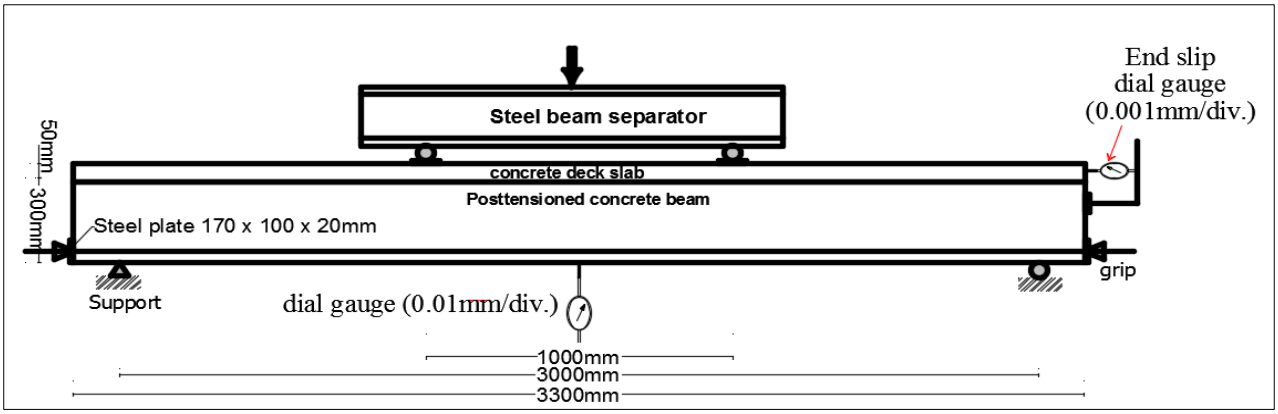


**Figure 3. Second test stage (loading test)**

## 5. Results and Discussion

### 5.1. Thermal Test Results

By using a digital thermometer reader with a thermocouple sensor wires type K and a dial gauge positioned at the top surface of deck slab at mid-span of the PC beam, the camber-time history was measured to find the change in the camber (upward deflection) during the burning and cooling periods.

The PC beams passed through three periods within the burning and cooling cycle. In the first period, the transition period to reach the target temperature of 300, 500, or 700˚C is approximately 20, 35, and 55 min, but the furnace reached these temperatures in 5, 10, and 15 min, respectively, as recommended by the standard fire curve (E119). Next, 1 h through the target temperatures. The temperature was controlled during the burning process by regulating the amount of methane gas reaching the nozzles. Finally, the fire flame was turned off, indicating the cooling period. The PC beams were cooled gradually by leaving the PC beams in the ambient air (lab condition). The effect of burning and cooling stages on the behaviour (mid-span camber) for all PC beams are summarized in Table 2.

Figures 4, 5, and 6 show the camber versus time history for the composite PC beams of Groups I, II, and III, respectively, through the burning and cooling processes. These Figures exhibit that increasing burning temperature lead to increase in the PC camber, despite the fire flam being positioned at the base of the furnace toward the lower cord of the PC beam. This may be due to the constitution of the PC beam that exhibits curvature (camber) due to the eccentric prestressing force, which compressed the concrete at the same cord of the prestressing force and stretching the other concrete cord. In other words, exposing a concrete beam to high temperature under sustained eccentric load increases the deteriorations, especially which of cord under tension stress. The structural response plotted in these Figures can be grouped into three periods, as mentioned earlier. In period 1, according to the standard fire E119, in the first 5, 10, or 15 min of fire exposure at the furnace temperatures of 300, 500, or 700˚C, respectively, the cambers in all PC beams increases at a slow pace, and these cambers result mainly from the thermal strains generated due to high thermal gradients that occur in the early stage of fire exposure. Concrete and strands undergo very little strength degradation in this stage due to the low temperatures in the concrete and strands. In contrast, this stage, according to the time needed to reach the PC beam to the same target temperature, which was 20, 35, or 55 min, respectively, the cambers in all PC beams increase at a high pace and these cambers result mainly from the thermal strains gained due to high thermal gradients that occur in the early stage of fire exposure.

In period 2, within 1 h at the target temperature into fire exposure, camber increased at a higher rate due to the reduction in the thermal concrete strength, as temperatures increase in the inner layers of concrete. The camber in this stage is mainly attributed to the degradation of strength and modulus in concrete more than that of strand due to increase in the sectional temperatures then cambers increase at a high pace, and this is mainly attributable to the high creep strains resulting from high temperatures in concrete, which is composed of different materials under the strand sustain load.

**Table 2. Camber at the end of each time period of burning and cooling stage for all PC beams**

| | Group. No. | First period | | Second period | | Third period | | Residual camber, % | Recovered camber % |
|---|---|---|---|---|---|---|---|---|---|
| | | Time, min. | Camber at mid span mm | Time, min. | Camber at mid span mm | Time, min. | Camber at mid span mm | | |
| Group I | B1-F20-R | - | | - | | - | | | |
| | B1-F20-300 | 20 | 1.5 | 80 | 1.9 | 300 | 1.6 | 145 | 19 |
| | B1-F20-500 | 35 | 1.7 | 95 | 2.6 | 450 | 1.8 | 164 | 44 |
| | B1-F20-700 | 55 | 2.4 | 115 | 4.2 | 580 | 3.3 | 300 | 27 |
| Group II | B2-F30-R | - | | | | | | | |
| | B2-F30-300 | 20 | 1.4 | 80 | 2.1 | 325 | 1.8 | 164 | 17 |
| | B2-F30-500 | 35 | 1.6 | 95 | 2.7 | 470 | 2.1 | 191 | 29 |
| | B2-F30-700 | 55 | 2.5 | 115 | 4.3 | 615 | 3.4 | 309 | 26 |
| Group III | B3-F40-R | - | | | | | | | |
| | B3-F40-300 | 20 | 1.4 | 80 | 2.2 | 340 | 2.0 | 182 | 10 |
| | B3-F40-500 | 35 | 1.6 | 95 | 2.9 | 495 | 2.2 | 200 | 32 |
| | B3-F40-700 | 55 | 2.6 | 115 | 4.4 | 640 | 3.6 | 327 | 22 |

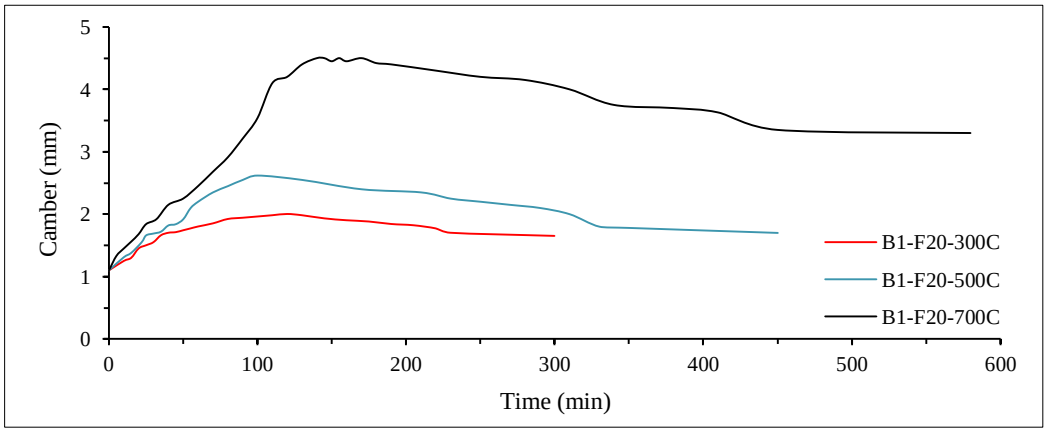


**Figure 4. Camber versus time history for PC beams of Group I at different burning temperatures (300, 500, and 700˚C)**

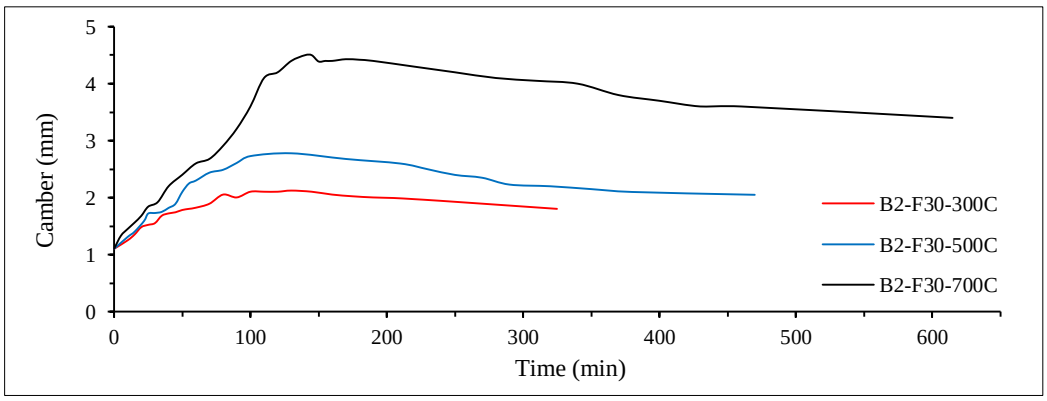


**Figure. 5. Camber versus time history for PC beams of Group II at different burning temperatures (300, 500, and 700˚ C)**

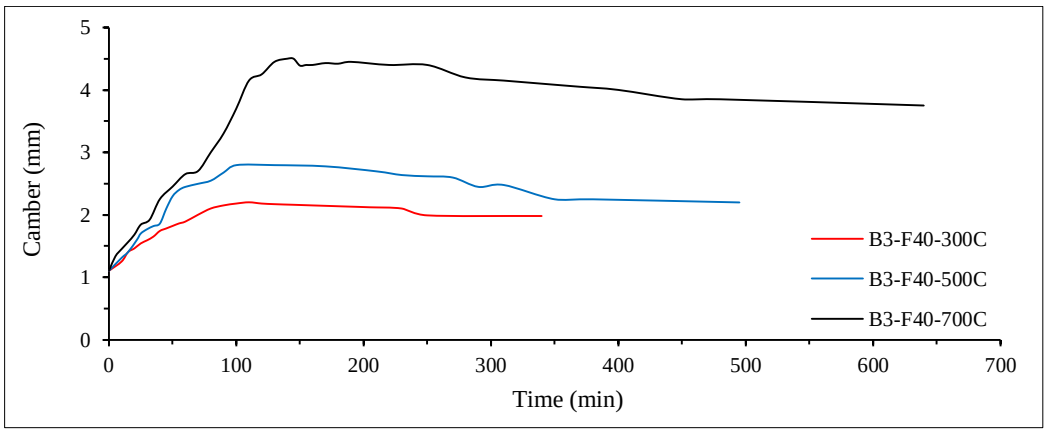


**Figure 6. Camber versus time history for PC beams of Group III at different burning temperatures (300, 500, and 700 ˚C)**

Table 6 shows the values of camber at the end of each time period. The table shows that, with increasing burning temperature, the camber of PC beam increased in all periods of burning and cooling cycle as well in the residual camber. At the end of the burning temperature (period 2) of 500 and 700˚C, the values were 137 and 221% for PC beams of Group I as compared to that burned at 300˚C. While, the values were 129 and 205% and 132 and 200% of Group II and III for the same burning temperatures, respectively.

At the end of the burning and cooling cycle (period 3), the residual camber for PC beams of Group I was 145, 164, and 300% for beams burned at 300, 500, and 700˚C, respectively, as compared to that of the initial camber before burning (1.1 mm). For PC beams of Groups II and III, the respective values were 164, 191, 309% and 182, 200, 327% for the abovementioned burning temperatures, respectively.

Comparing the effect of top flange concrete strength, where the PC beams have identical concrete strength, revealed that, with increasing concrete strength of the top flange, the deterioration increases at the same burning circumstance. Exposed PC beams topped with flange had 30 and 40 MPa concrete strength at 300˚C burning, which indicates that, increase in the maximum camber at the end of the burning temperature occurs by 11% and 15% and the residual final camber at the end of cooling period by 13 and 25%, respectively, as compared to those of PC beam topped with flange concrete strength of 20 MPa. On the other hand, the respective values were 4 and 16% and 17 and 22% for Group II and 2 and 105% and 103 and 109% for Group III at the burning temperatures of 500 and 700˚C, respectively.

These comparisons reflect the defects occurring due to exposure of the PC beams to fire flame (Figure 7). It can be seen from this Figure that, for each group (same PC beams properties), increase in the burning temperature leads to increase in the residual final camber, which reflects the amount of burning damage, and increase in the concrete strength lead to increase in the defects due to increase in the concrete density and decrease in the porosity.

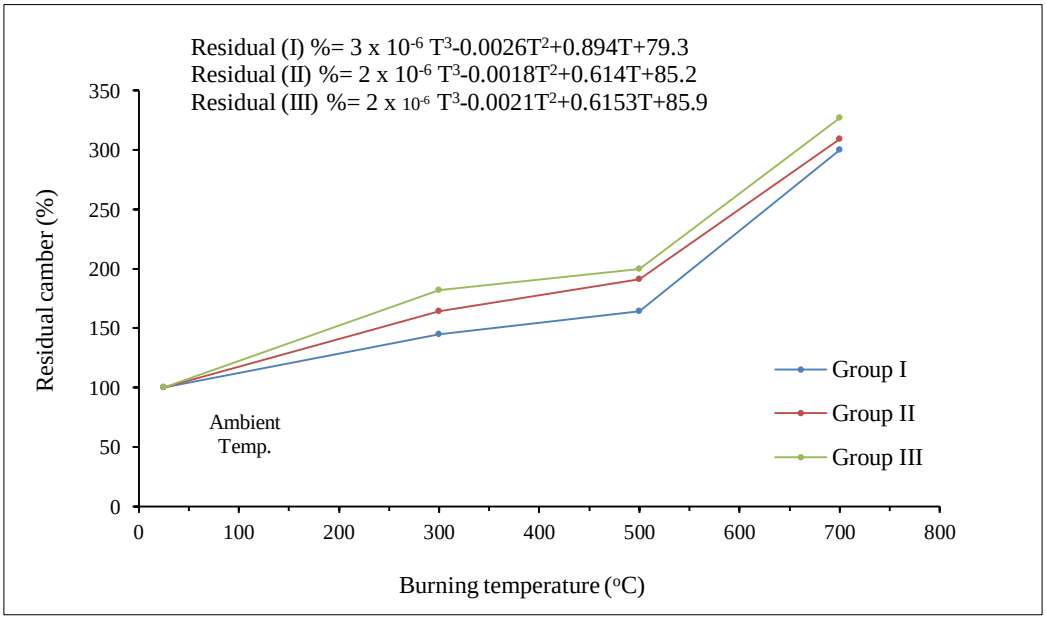


**Figure 7. Residual final camber at the end of burning and cooling cycle versus burning temperature, for each group**

The difference in behaviour (camber) of beams at each group is shown in Figures 4 to 6, which is an indication of the normal variability associated with different lengths of period for fire test and temperature burning. The camber increases during heating period and reaches the maximum at the end of the burning period. The upward movement of the PC beam can probably be explained by reduction in the concrete resistance at the location of cracking and spalling, such that the residual force in the prestressing tendons causes the beam to move upwards.

The comparisons shown in Figures 8-10 exhibit the different effect of the top flange concrete strength on the camber throughout the burning and cooling periods. As mentioned earlier, increasing concrete strength leads to increase in the deteriorations and crack formation due to increase in the concrete density of the concrete past.

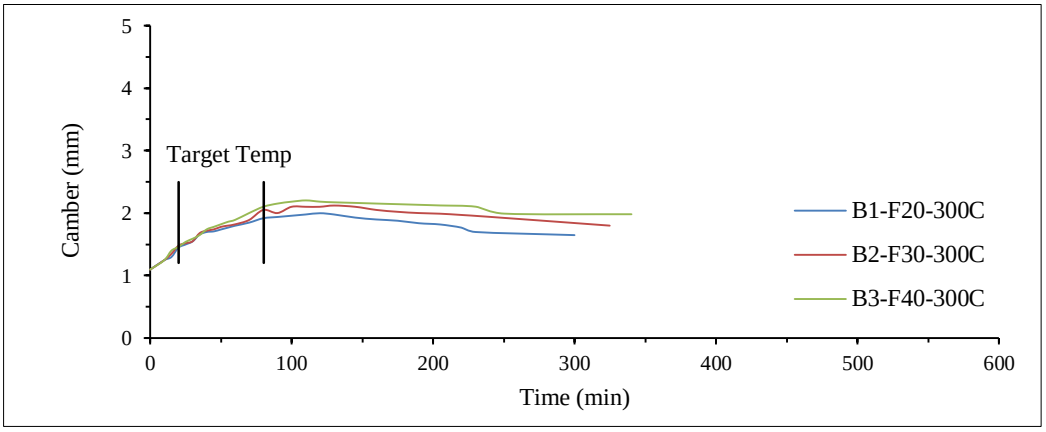


**Figure 8. Camber-time history of burned PC beams with different flange concrete strengths at 300˚C**

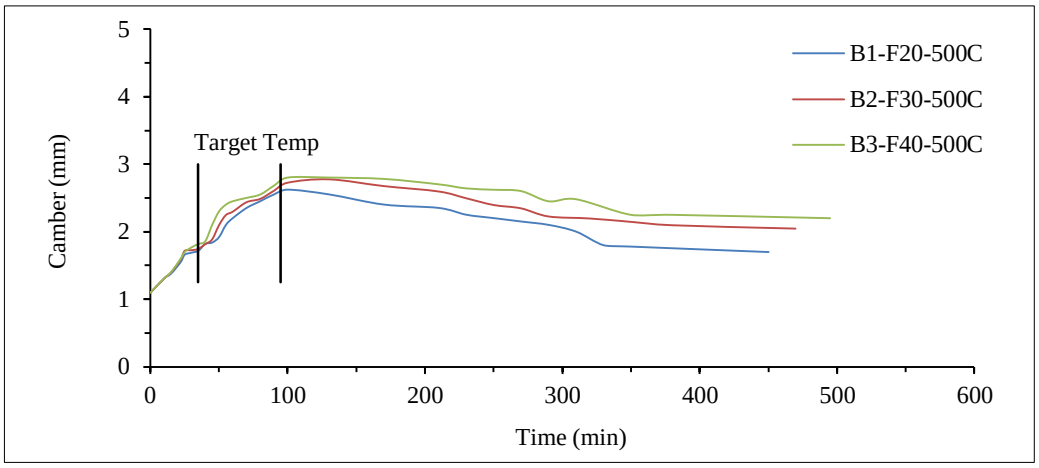


**Figure 9. Camber-time history of burned PC beams with different flange concrete strengths at 500˚C**

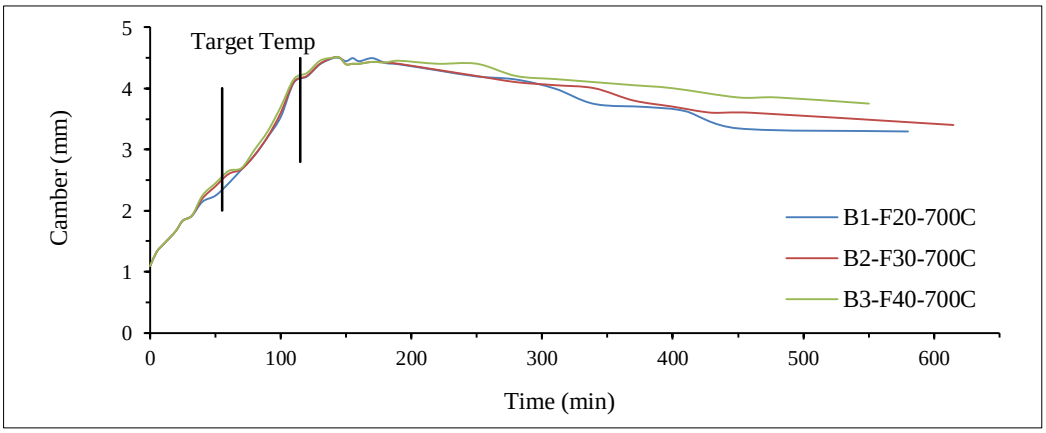


**Figure 10. Camber-time history of burned PC beams with different flange concrete strengths at 700˚C**

## 5.2. Load-Deflection Relations

Figures 11-13 show the load-deflection curves for the post-fire composite PC beams of Groups I-III, respectively. It can be noted that, the exposure to fire temperature decreases the load-carrying capacity of composite PC beams. This can be attributed to the fact that heating causes a reduction in the beam stiffness, which is essentially due to the reduction in the modulus of elasticity of concrete and the reduction in the effective section due to cracking. The general load versus mid-span deflection behaviours of reference composite PC beams and of that burned at 300°C were approximately similar. On the other hand, for post-fire PC beams burned at 500 and 700 °C, the load versus mid-span deflection relations indicated softer behaviours in general as compared with those of the reference composite PC beams. This can be attributed to the weaker bond strength between the concrete and steel reinforcement or decomposition of the concrete components itself. Moreover, the flatten load-deflection relations of PC beams exposed to fire flame with that of the reference beams can be attributed to the early crack formation and lower modulus of elasticity. It should be noted that all beams exposed to fire were cracked before commencement of the load test, unlike for the beams not exposed to fire.

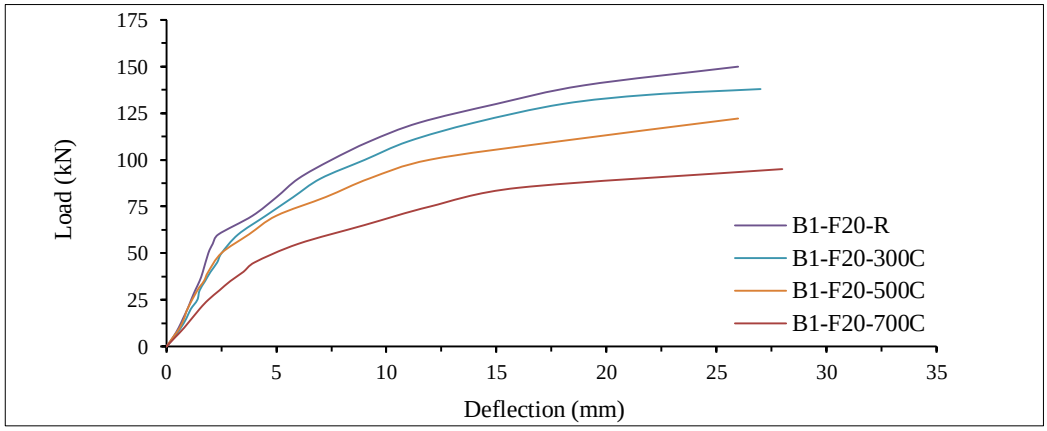


**Figure 11. Load-deflection curve of Group I**

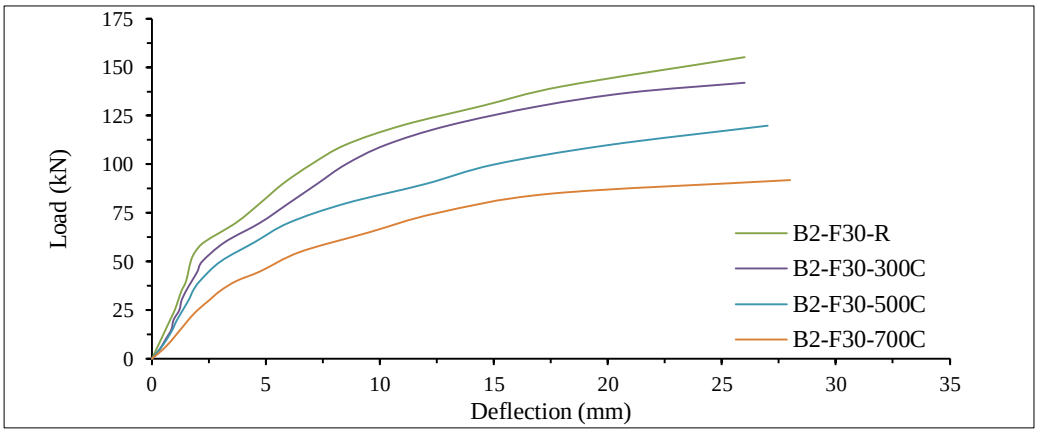


**Figure 12. Load-deflection curve of Group II**

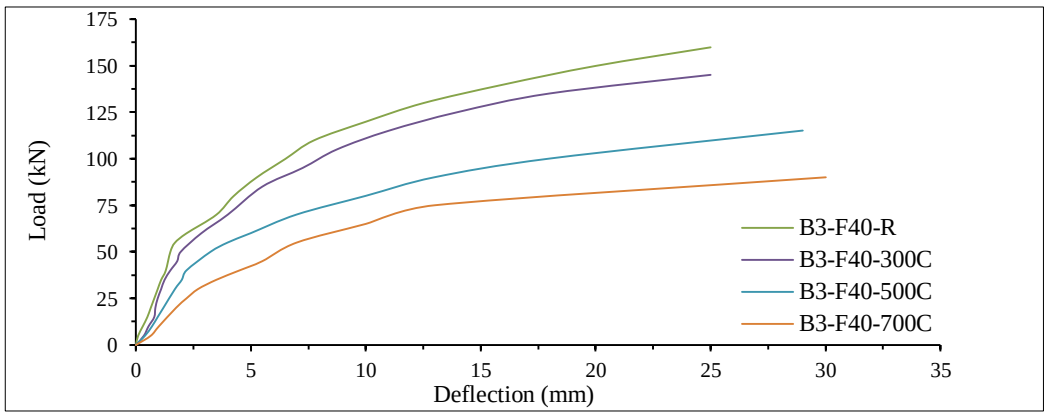


**Figure 13. Load-deflection curve of Group III**

Table 3 shows the value of load and corresponding deflection at the first visible crack for reference PC beams and at failure for all composite PC beams. The test results revealed that visible first crack for the reference PC beams was at load 60 kN, accordingly, the applied load of 50 kN was selected within the service limit of PC beams, and, out of this range, the load corresponding to the 20 mm deflection was chosen to build comparisons. As shown in this table and in Figures 14 and 15, with increasing burning temperature, the deflection increases. This increment was excessive with increasing burning temperatures at ≥500ºC. At the applied load of 50 kN, the ratio of the burned to unburned PC beams deflection topped with concrete flange strength of 20, 30, and 40 MPa and to those exposed to the burning temperature of 300ºC was 126, 129, and 130%, respectively. The different increases for a similar comparison, but for the PC beams burned at 500 and 700ºC was 137, 176, and 220%, and 263, 329, and 420%, respectively. Figure 14 shows that, until about 300ºC, the concrete strength of top flange had an approximate similar ratio of burned to unburned deflection, while this ratio was deviated at 500 and 700ºC. The same behavior was observed at the applied load near the ultimate resistance corresponding to the 20 mm deflection (Figure 15).

The comparisons shown in Figures 16-19 exhibited the effect of the top flange concrete strength on the load-deflection curves for the post-fire composite PC beams during the static load test. These Figures exhibit that, up to the burning temperature of 300ºC, increasing concrete strength enhances the stiffness of PC beams. In contrast, increase in the concrete strength led to decrease in the load-deflection curves (stiffness) in the burned composite PC beams by more than that. As mentioned earlier, increasing concrete strength led to increase in the deteriorations and crack formation due to increase in the concrete density of the concrete past, resulting in more reduction in the beam stiffness.

**Table 3. Cracking, Yielding, Ultimate Load and The Corresponding Deflections for all Composite PC Beams**

| | | Crack Limit | | At 50kN load | | At 20mm deflection | | Ultimate Limit | |
|---|---|---|---|---|---|---|---|---|---|
| | Group No. | Crack Load, KN | Crack deflection, mm | Deflection, mm | Deflection ratio of burned /unburned, % | Resistance load kN | Load ratio of burned /unburned, % | Ultimate Load, kN | Ultimate Deflection, mm |
| Group I | B1-F20-R | 60 | 2.35 | 1.9 | 100 | 141 | 100 | 150 | 26 |
| | B1-F20-300 | - | - | 2.4 | 126 | 132 | 94 | 138 | 27 |
| | B1-F20-500 | - | - | 2.6 | 137 | 113 | 80 | 122 | 26 |
| | B1-F20-700 | - | - | 5.0 | 263 | 89 | 63 | 95 | 28 |
| Group II | B2-F30-R | 60 | 2.3 | 1.7 | 100 | 144 | 100 | 155 | 26 |
| | B2-F30-300 | - | - | 2.2 | 129 | 135 | 94 | 142 | 26 |
| | B2-F30-500 | - | - | 3.0 | 176 | 110 | 76 | 120 | 27 |
| | B2-F30-700 | - | - | 5.6 | 329 | 85 | 59 | 92 | 28 |
| Group III | B3-F40-R | 60 | 2.2 | 1.5 | 100 | 150 | 100 | 160 | 25 |
| | B3-F40-300 | - | - | 1.95 | 130 | 137 | 91 | 145 | 25 |
| | B3-F40-500 | - | - | 3.3 | 220 | 103 | 69 | 115 | 29 |
| | B3-F40-700 | - | - | 6.3 | 420 | 81 | 54 | 90 | 30 |

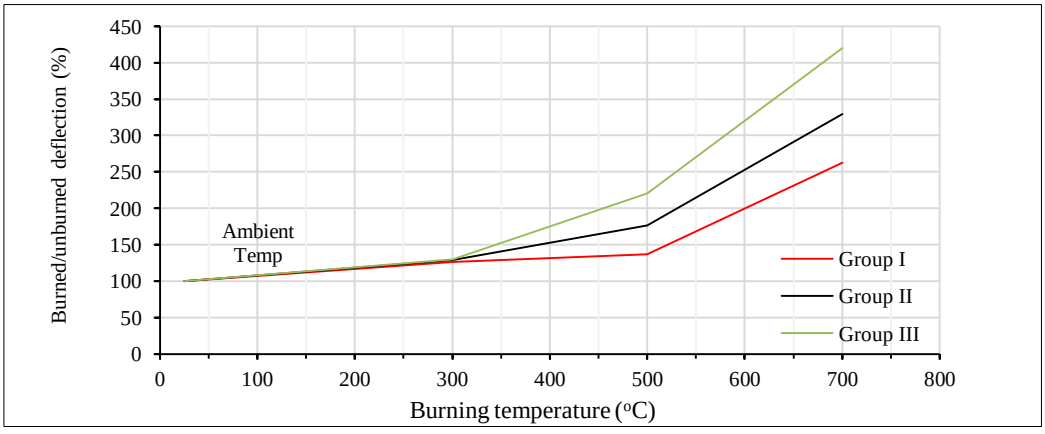


**Figure 14. Effect of temperature on the deflection at applied load of 50kN**

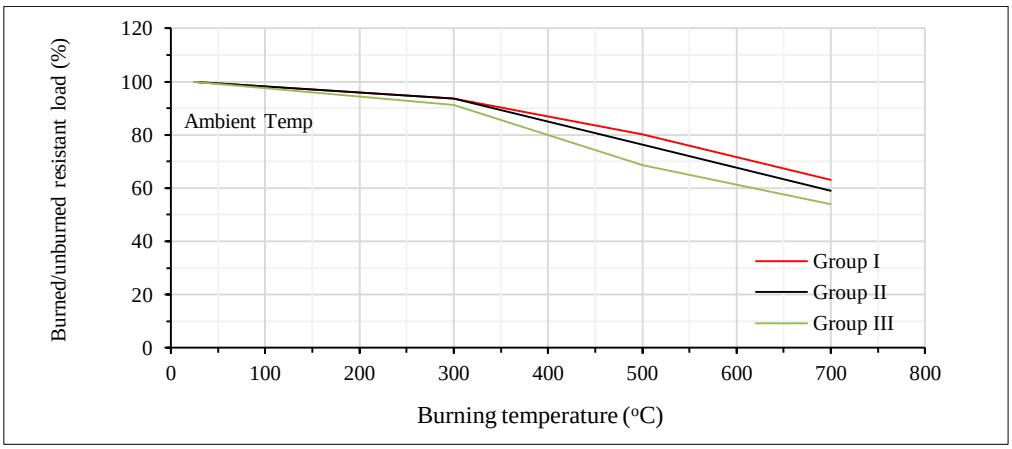


**Figure 15. Effect of temperature on the resistant load at deflection of 20 mm**

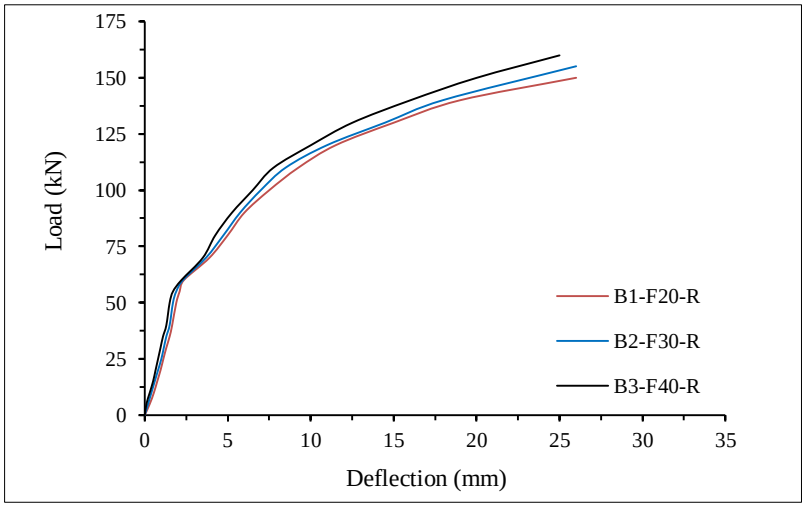


**Figure 16. Load-deflection curves for unburned composite PC beams with different flange concrete strengths**

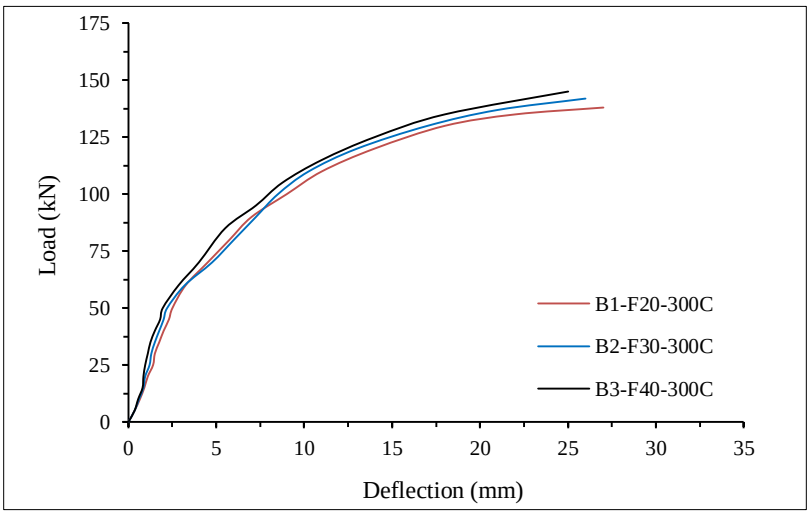


**Figure 17. Load-deflection curves for burned composite PC beams with different flange concrete strengths at burning temperature 300˚C**

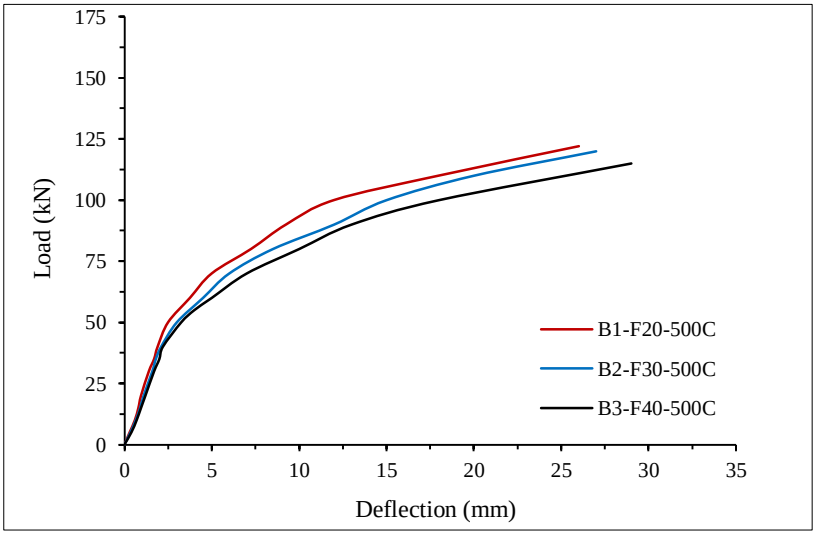


**Figure 18. Load-deflection curve for burned composite PC beams with different flange concrete strengths at burning temperature 500˚C**

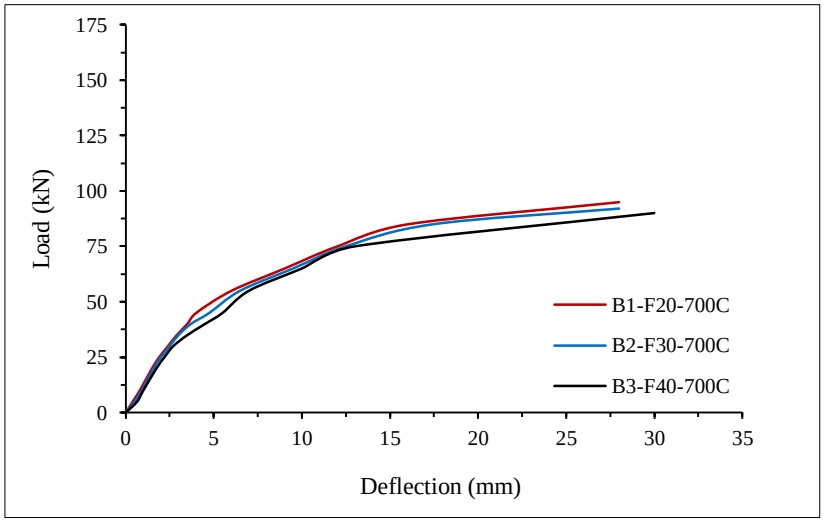


**Figure 19. Load-deflection curve for burned composite PC beams with different flange concrete strengths at burning temperature 700˚C**

## 5.3. Failure Mode and Load Carrying Capacity

Table 4 and Figure 20 show the effect of high temperature on the ultimate load capacity for all PC composites. The test results listed in this table reveal that, the values of load-carrying capacity decreased when the beams were exposed to a burning temperature of 300, 500, and 700ºC. This observation can be attributed to the fact that heating causes a reduction in the beam stiffness, which is essentially due to the reduction in the modulus of elasticity of concrete and the reduction in the effective section due to cracking. For PC beams topped with flange with a compressive strength of 20 MPa (Group I), the residual load-carrying capacity was 92, 81, and 63% for the burning temperatures of 300, 500, and 700ºC, respectively, as compared with its reference composite PC beam. On the other hand, the values were 92, 77, and 59% and 91, 72, and 56% for the same burning temperatures, but PC beams topped with flange had compressive strengths of 30 and 40 MPa, respectively.

Figure 21 A comparison of the effect of top flange concrete strength, where the prestressed concrete beam showed similar concrete strength, indicating that, in contrast to the reference PC beams and those burned at temperature up to 300ºC, increasing concrete strength of the top flange led to increased reduction in the load-carrying capacity at the same burning situation. At the burning temperature of 300ºC, increase in the load-carrying capacity was 103 and 105% for the composite PC beams of 30 and 40 MPa top flange concrete strength, respectively, as compared to that of 20 MPa top flange concrete strength, which showed approximately the same values as that of the reference PC beams (103 and 107%, respectively) for the same top concrete flange strength. Meanwhile, at a burning temperature of 500ºC, the residual load-carrying capacity was 98 and 94% for the composite PC beams of 30 and 40 MPa top flange concrete strength, respectively, while they were 97 and 95% for the same top flange compressive strength but at 700ºC burning

temperature compared to those of 20 MPa top flange concrete strength. It can be concluded that the increase in the concrete compressive strength for the top flange of composite PC beam had a slight increasing effect on the ultimate load-carrying capacity, because of the slight variation in the depth of compressive zone for composite PC beams. In contrast, at high burning temperatures, increase in the concrete strength had a reverse effect.

**Table 4. Ultimate load capacity and mode of failure of Composite PC beams**

| | Group | Ultimate Load (kN) | Burned/ Unburned % | Failure Mode |
|---|---|---|---|---|
| Group I | B1-F20-R | 150 | 100 | Yielding and concrete crushing |
| | B1-F20-300 | 138 | 92 | Rupture of steel reinforcements and concrete crushing |
| | B1-F20-500 | 122 | 81 | Rupture of reinforcing steel bars and concrete crushing |
| | B1-F20-700 | 95 | 63 | Rupture of prestressing strand and reinforcing steel bars |
| Group II | B2-F30-R | 155 | 100 | Yielding and concrete crushing |
| | B2-F30-300 | 142 | 92 | Rupture of steel reinforcements and concrete crushing |
| | B2-F30-500 | 120 | 77 | Rupture of reinforcing steel bars and concrete crushing |
| | B2-F30-700 | 92 | 59 | Rupture of prestressing strand and reinforcing steel bars |
| Group III | B3-F40-R | 160 | 100 | Yielding and concrete crushing |
| | B3-F40-300 | 145 | 91 | Yielding and concrete crushing |
| | B3-F40-500 | 115 | 72 | Rupture of prestressing strand and reinforcing steel bars |
| | B3-F40-700 | 90 | 56 | Rupture of prestressing strand and reinforcing steel bars |

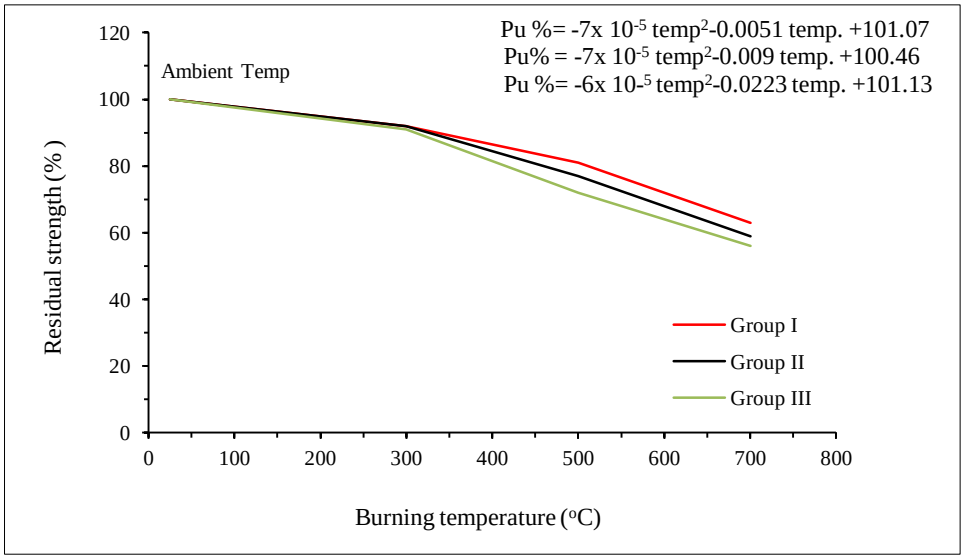


**Figure 20. Burning effect of PC beams on residual strength**

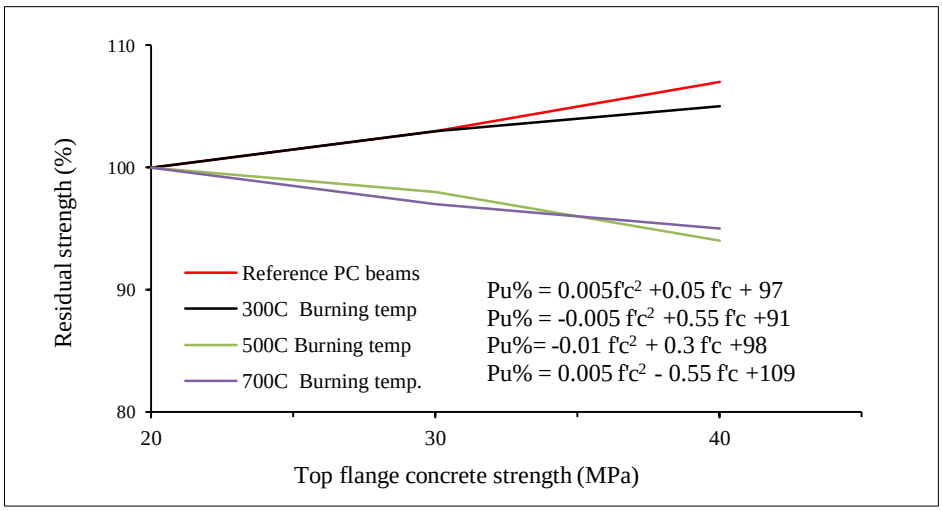


**Figure 21. Effect of top flange concrete strength on residual strength**

Figures 22 to 24 demonstrate the failure mode for unburned and burned composite PC beams at deferent burning temperatures and concrete strength of beam top flange. Generally, two types of failures occurred, yielding reinforcement in tension (prestressed strand or reinforcing steel or both), followed by compression failure of concrete and rupture of steel (prestressed strand or reinforcing steel or both) after crushing of concrete (Table 4).

Reference beams (B1-F20, B2-F30, and B3-F40) failed to yield reinforcement in tension (reinforcing steel bar), followed by compression failure of concrete. Initially, failure stage started with mid-span deflection, followed by flexural cracks along the beam bottom when the applied load reached the crack load. Some of these flexural cracks at the middle zone propagated toward the compression cord of the composite PC beam. As the applied load increased, additional cracks formed throughout and continued widening and propagating until failure (composite PC beam could not resist any further applied load), as shown in Figure 22.

The failure of burned composite PC beams (B1-F20, B2-F30, and B3-F40) at the burning temperature of 300˚C were the same as that for the reference beams in yielding and rupturing of steel (reinforcing steel bars), with crushing of concrete for the composite PC beams B1-F20 and B2-F30 and in yielding of the reinforcement in tension (reinforcing steel bar), followed by compression failure of concrete for the composite PC beam B3-F40. However, due to the burning and cooling processes, the PC beam and top flange suffered from some flexural cracks initiated before applying the static load, which increased in length and width with the increasing load. Therefore, it was difficult to distinguish the new cracks. On the other hand, the mid-span deflection appeared to be slightly larger at the same applied load and visible flexural cracks from along the beam bottom face formed at less load than that of reference PC beams. Some cracks rapidly propagated to the top cord of the composite PC beam and increasing mid-span deflection, causing failure. Heating causes a reduction in the stiffness, ductility, and in the flexural capacity in composite PC beam compare with reference composite PC beam.

The failure of burned composite PC beams at burning temperatures of 500 and 700˚C were in rupture of steel (reinforcing steel bars and strand) with crushing of concrete. When applied with a load, the mid-span deflection appeared larger at the same applied load and visible flexural cracks from along the beam bottom face formed more in length and width at less load as compared with that of composite PC beams at a burning temperature of 300˚C. Cracks rapidly propagated to the top cord of the composite PC beam and increasing mid-span deflection occurred, causing failure. The increase in the burning temperature causes increasing reduction in stiffness, ductility, and in the flexural capacity in composite PC beam as compared to that in the reference PC beams. Figure 23 shows the failure of the burned composite PC beam (B1-F20, B2-F30, and B3-F40) at the burning temperature of 500˚C.

No slippage was detected by the dial gauge fixed at the end of the beam (Figure 3), in the references composite PC beams because sufficient shear connector reinforcements were possibly used than with the post-fire composite PC beams, because the two composite layers deteriorated and lost much of their rigidities at different places other than the ends.

**(a) Failure mode of B1-F20-R** **(b) Failure mode of B2-F30-R** **(c) Failure mode of B3-F40-R.**

**Figure 22. Failure mode of unburned composite PC beams**

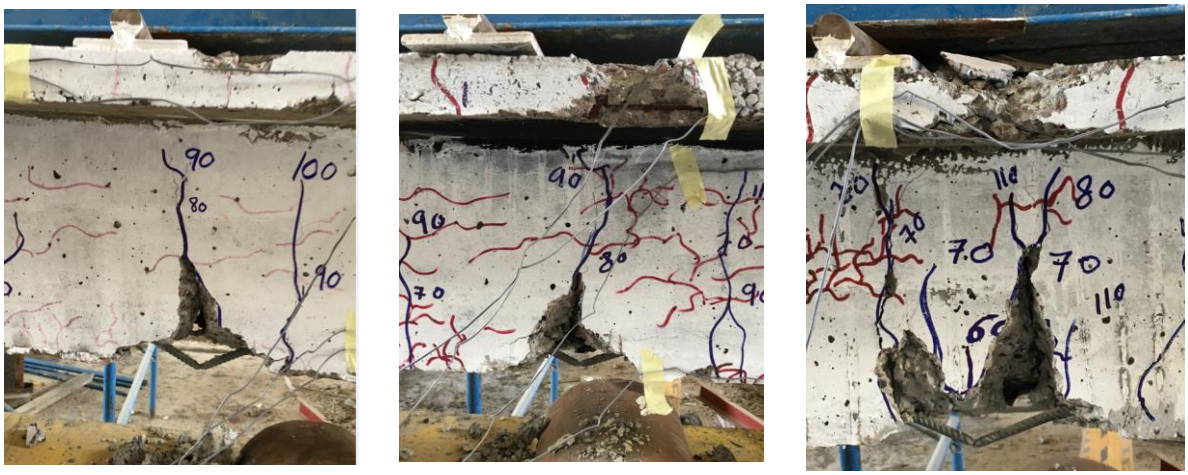

**(a). Failure mode of B1-F20-500 ºC** **(b). Failure mode of B2-F30-500 ºC** **(c). Failure mode of B3-F40-500 ºC**

**Figure 23. Failure mode of composite PC beams burned at 500 ºC**

## 6. Conclusions

- Increasing the burning temperature leads to increase in the camber of composite PC beam at all periods of burning and cooling cycle as well the residual camber. At the end of burning at temperatures of 500 and 700˚C, the camber values were 137 and 221% for PC beams of Group I as compared to that burned at 300˚C. On the other hand, the respective values were 129 and 205% and 132 and 200% for Group II and III at the same burning temperatures.
- At the end of the burning and cooling cycle, the residual camber for PC beams of Group I was 145, 164, and 300% for burned beams at 300, 500, and 700˚C, respectively, as compared to the initial camber before burning (1.1 mm). While, for PC beams of Group II and II, it was 164, 191, and 309% and 182, 200, and 327%, for the same above burning temperatures, respectively.
- Increasing concrete strength of the top flange, whereas the PC beam had identical concrete strength, the deterioration increased at the same burning circumstance. Exposing PC beams topped with flange had 30 and 40 MPa concrete strength to 300˚C, reveals that increase in the maximum camber at the end of the burning temperature by 11 and 15% and the residual final camber at the end of cooling period by 13 and 25%, respectively, as compared to PC beam topped with flange concrete strength of 20 MPa. While, it was 4 and 16% and 17 and 22% for Group II and 2 and 105% and 103 and 109% for Group III at the burning temperatures of 500 and 700˚C, respectively.
- The exposure to fire temperature decreases the beam stiffness of PC beams. At ambient temperature and 300°C, the general load versus mid-span deflection behaviour was approximately similar. On the other hand, for burning temperatures 500 and 700°C, this relation was softer and more flat than for those of the reference composite PC beams. This finding can be attributed to the early crack formation and lower modulus of elasticity. It should be noted that all the beams exposed to fire were cracked before commencement of the load test unlike for the beams not exposed to fire.
- The load-carrying capacity decreases when the beams are exposed to burning temperature. For PC beams topped with flange of compressive strength 20 MPa (Group I), the residual load-carrying capacity was 92, 81, and 63% for burning temperatures 300, 500, and 700ºC, respectively, as compared with its unburned (reference) composite PC beam. While, for that topped with 30 MPa flange compressive strength, the residual load-carrying capacity was 92, 77, and 59% for the same burning temperatures, respectively, On the other hand, for PC beams topped with flange of compressive strength 40 MPa, the residual load-carrying capacity was 91, 72, and 56% for burned beams at 300, 500, and 700ºC as compared with those of the reference composite PC beam.
- Increase in concrete compressive strength for the top flange of composite PC beam showed a slightly increased effect on the ultimate load-carrying capacity, because of a little variation in the depth of compressive zone for composite PC beams. In contrast, at high burning temperatures, increasing concrete strength has a reverse effect.
- The failure mode demonstrates that the unburned (reference) and burned beams at 300ºC failed in yielding reinforcement in tension (reinforcing steel bar), followed by compression failure of concrete. In addition, the composite PC beams burned at 500 and 700˚C were in rupture of steel (reinforcing steel bar) after crushing of concrete. Moreover, the mode of failure of post-fire composite PC beams is more ductile than that of unburned ones.

## 7. References

[1] Chang, Y.F., Y.H. Chen, M.S. Sheu, and G.C. Yao. "Residual Stress–strain Relationship for Concrete after Exposure to High Temperatures." Cement and Concrete Research 36, no. 10 (October 2006): 1999–2005. doi:10.1016/j.cemconres.2006.05.029.

[2] Youssef, M.A., and M. Moftah. "General Stress–strain Relationship for Concrete at Elevated Temperatures." Engineering Structures 29, no. 10 (October 2007): 2618–2634. doi:10.1016/j.engstruct.2007.01.002.

[3] Alarcon-Ruiz, Lucia, Gerard Platret, Etienne Massieu, and Alain Ehrlacher. "The Use of Thermal Analysis in Assessing the Effect of Temperature on a Cement Paste." Cement and Concrete Research 35, no. 3 (March 2005): 609–613. doi:10.1016/j.cemconres.2004.06.015.

[4] Ghani, U., Shabbir, F., and Khan, K. M. "Effect of temperature on different properties of concrete." 31st Conference on Our World in Concrete and Structures, Singapore, (2006): 16-17.

[5] Hedayati, M., Mendis, P. A., Sofi1, M.; and Ngo, T.. Fire spalling of concrete members. 6th International Conference on Structural Engineering and Construction Management, Kandy, Sri Lanka, (2015): 204-210.

[6] Pierre,K., Menneteau F.D., and Quenard .D., "Spalling and Pore Pressure in HPC at High Temperatures." Cement and Concrete Research 30, no. 12 (December 2000): 1915–1927. doi:10.1016/s0008-8846(00)00384.

[7] Britain, G." Fire resistance of concrete structures: report of a Joint Committee of the Institution of Structural Engineers and the Concrete Society", London: Institution of Structural Engineers (1975).

[8] Hertz, K.D., and L.S. Sørensen. "Test Method for Spalling of Fire Exposed Concrete." Fire Safety Journal 40, no. 5 (July 2005): 466–476. doi:10.1016/j.firesaf.2005.04.001.

[9] Aslani, Farhad. "Prestressed Concrete Thermal Behaviour." Magazine of Concrete Research 65, no. 3 (February 2013): 158–171. doi:10.1680/macr.12.00037.

[10] Myers, J. J., and Bailey, W.L. "SEVEN-WIRE LOW RELAXATION PRESTRESSING TENDON SUBJECTED TO EXTREME TEMPERATURES: RESIDUAL PROPERTIES". International journal of engineering research and science and technology. No.3(2015) : 223-239.

[11] Chen, J., and Young, B."Mechanical properties of cold-formed steel at elevated temperatures", presented at 17th International Specialty Conference on Cold-Formed Steel Structures, Missouri University of Science and Technology (2004).

[12] Fletcher, I., Welch, S., Torero, J., Carvel, R., and Usmani, A. "Behaviour of Concrete Structures in Fire." Thermal Science 11, no. 2 (2007): 37–52. doi:10.2298/tsci0702037f.